

# Dissecting Competitive Mechanisms: Thionation vs. Cycloaddition in the Reaction of Thioisomünchnones with Isothiocyanates under Microwave Irradiation<sup>†</sup>

David Cantillo,<sup>\*,‡</sup> Martín Ávalos,<sup>‡</sup> Reyes Babiano,<sup>‡</sup> Pedro Cintas,<sup>‡</sup> José L. Jiménez,<sup>‡</sup> Mark E. Light,<sup>§</sup> and Juan C. Palacios<sup>‡</sup>

<sup>‡</sup>Departamento de Química Orgánica e Inorgánica, QUOREX Research Group, Facultad de Ciencias, Universidad de Extremadura, E-06071 Badajoz, Spain, and <sup>§</sup>Department of Chemistry, University of Southampton, Highfield, Southampton SO17 1BJ, United Kingdom

dcannie@unex.es

Received May 8, 2009



This paper documents in detail the reaction of 1,3-thiazolium-4-olates (thioisomünchnones) with aryl isothiocyanates. Having demonstrated with a chiral model that thionation occurs under these conditions to provide 1,3-thiazolium-4-thiolates and that this process is actually a stepwise domino reaction (*J. Org. Chem.* **2009**, *74*, 3698–3705), we extend this study to monocyclic thioisomünchnones. Herein, competition between thionation and 1,3-dipolar cycloaddition takes place. The process is synthetically disappointing at room temperature requiring prolonged reaction times for completion. The protocol has been subsequently investigated by using both microwave dielectric heating and conventional thermal heating (oil bath) in DMF at 100 °C with an accurate internal reaction temperature measurement. Although a slight acceleration was observed for reactions conducted under microwave irradiation, for most cases the observed yields and chemoselectivities were quite similar. Thus one can conclude that, within experimental errors, the reactivity is not related to nonthermal effects in agreement with recent reassessments on this subject, particularly by Kappe and associates (*J. Org. Chem.* **2008**, *73*, 36; *J. Org. Chem.* **2009**, *74*, 6157). The whole reaction system, which includes numerous heavy atoms, can be computationally modeled with a hybrid ONIOM[B3LYP/6-31G(d):PM3] level. This reproduces well experimental results and suggests a sequential mechanism. To further corroborate the nonconcertedness, the potential energy surface (PES) has been constructed for simplified models, locating the corresponding stationary points. In doing so, we introduce for the first time a useful and convenient mathematical protocol to locate the stationary points along a reaction path. The protocol is quite simple and should convince many organic chemists that certain daunting theoretical treatments can be made easy.

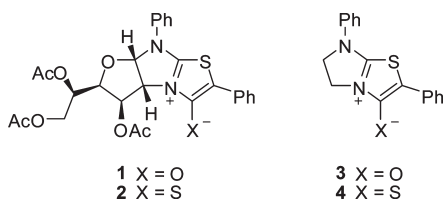
## Introduction

During the past few decades there has been a growing interest in synthetic strategies based on the 1,3-dipolar reactivity of mesoionic heterocycles, leading to novel heterocyclic scaffolds as well as natural products or their analogues.<sup>1</sup> Also, in recent years these fascinating heterocycles have been considered for nonlinear optics on the basis of their large hyper-

polarizabilities, the relative ease of their synthesis, and the possibility of tailoring the associated optical properties by manipulation of their chemical structure.<sup>2</sup> However, the required stability of NLO materials limits the use of mesoionic systems, unless it can be enhanced by a suitable exchange of the electron-withdrawing exocyclic atoms, namely incorporation of a heavier sulfur atom. Several synthetic procedures, including tandem cycloaddition–retrocycloaddition processes,<sup>3</sup> alkylation with a trialkyloxonium salt followed by the replacement of the resulting alkoxy group by sulfide or

<sup>†</sup> Dedicated to Prof. Luis Castedo on celebrating his 70th birthday.

hydrogen sulfide anion,<sup>4</sup> or the treatment with Lawesson's reagent,<sup>5</sup> have been so far described for the conversion of mesoionic olates into mesoionic thiolates. In this context we have recently reported the conversion of imidazo[2,1-*b*]thiazolium-3-olate systems (**1** and **3**) into the corresponding imidazo[2,1-*b*]thiazolium-3-thiolate derivatives (**2** and **4**) by reaction with aryl isothiocyanates, and proving unequivocally that this thionation does actually proceed via a domino mechanism.<sup>6</sup>

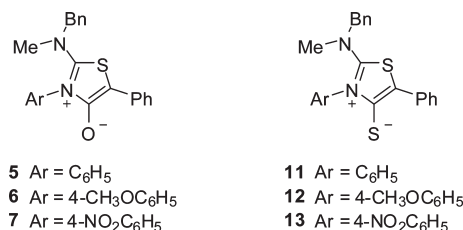


To delineate the scope of this methodology, it is convenient to move it from fused and polycyclic systems to the more readily available monocyclic 1,3-thiazolium-4-thiolates. Furthermore, this study should allow us to disentangle the fate of two competing processes, i.e., thionation and the expected cycloaddition of the masked dipole with the heterocumulenic partner. In the course of this theoretical research, we came across a simple and intuitive protocol for the location of all stationary points along the potential surface. This methodology is described in detail and we judge many synthetic chemists will find it both useful and computationally inexpensive, thus overcoming the fears in moving from the bench to virtual chemistry.

## Results and Discussion

**Syntheses and Reactivity.** The reaction of monocyclic 3-aryl-2-dialkylaminothioisomünchnones with aryl isothiocyanates leads to 3-aryl-2-dialkylamino-1,3-thiazolium-4-thiolates. This O/S exchange occurs through two competitive reaction pathways, a thionation process similar to that described for the synthesis of **2** and **4**, which retains the aryl group on N-3, and a domino cycloaddition–retrocycloaddition process that adds the aryl group from isothiocyanate to the new mesoionic structure. Obviously, only one thiolate system is obtained when the aryl groups of both reaction partners are identical.

Thus, mesoionic heterocycles **5–7** react with phenyl, 4-methoxyphenyl, and 4-nitrophenyl isothiocyanates (**8–10**) to afford the corresponding mixtures of 3-aryl-2-(*N*-methylbenzylamino)-5-phenyl-1,3-thiazolium-4-thiolate systems **11–13**. Initially, such reactions were carried out in CH<sub>2</sub>Cl<sub>2</sub> at room temperature by using a 1:5 ratio of thioisomünchnone–isothiocyanate, and compounds **11–13** could be isolated by column chromatography by using benzene–acetonitrile gradients after no more than 48 h. The low yields thus obtained were increased when DMF was used as solvent (Table 1). A further improvement was achieved by conducting these transformations in DMF at 100 °C (oil bath) leading to completion in less than 40 min.



(1) (a) Potts, K. T. In *1,3-Dipolar Cycloaddition Chemistry*; Padwa, A.; Wiley: New York, 1984; Vol. 2, pp 1–82. (b) Ollis, W. D.; Stanforth, S. P.; Ramsden, C. A. *Tetrahedron* **1985**, *41*, 2239. (c) Osterhout, M. H.; Nadler, W. R.; Padwa, A. *Synthesis* **1994**, 123–141. (d) Padwa, A. *Top. Curr. Chem.* **1997**, *189*, 121–158. (e) Gribble, G. W. In *Synthetic Applications of 1,3-Dipolar Cycloaddition Chemistry Toward Heterocycles and Natural Products*; Padwa, A., Pearson, W. H., Eds.; Wiley: New York, 2003; pp 681–753. (f) Gribble, G. W. In *The Chemistry of Heterocyclic Compounds*; Vol. 60. Oxazoles: Synthesis Reactions and Spectroscopy, Part A; Palmer, D. A., Ed.; Wiley: New York, 2003; Chapter 4. (g) Dhawan, R.; Dghaym, R. D.; Arndtsen, B. A. *J. Am. Chem. Soc.* **2003**, *125*, 1474–1475. (h) Avalos, M.; Babiano, R.; Cintas, P.; Jiménez, J. L.; Palacios, J. C. *Acc. Chem. Res.* **2005**, *38*, 460–468. (i) Lu, Y.; Arndtsen, B. A. *Angew. Chem., Int. Ed.* **2008**, *47*, 5430–5433.

(2) (a) Morley, J. O. *J. Phys. Chem.* **1995**, *99*, 1923–1927. (b) Moura, G. L. C.; Simas, A. M.; Miller, J. *Chem. Phys. Lett.* **1996**, *257*, 639–646. (c) Bezerra, A. G. Jr.; Gomes, A. S. L.; Athayde-Filho, P. F.; Rocha, G. B. da; Miller, J.; Simas, A. M. *Chem. Phys. Lett.* **1999**, *309*, 421–426. (d) Menezes, L. de S.; Araújo, C. B. de; Alencar, M. A. R. C.; Athayde-Filho, P. F.; Miller, J.; Simas, A. M. *Chem. Phys. Lett.* **2001**, *347*, 163–166. (e) Pilla, V.; Araújo, C. B. de; Lira, B. F.; Simas, A. M.; Miller, J.; Athayde-Filho, P. F. *Opt. Commun.* **2006**, *264*, 225–228. (f) Bosco, C. A. C.; Maciel, G. S.; Rakov, N.; Araújo, C. B. de; Acioli, L. H.; Simas, A. M.; Athayde-Filho, P. F.; Miller, J. *Chem. Phys. Lett.* **2007**, *449*, 101–106.

(3) (a) Huisgen, R.; Funke, E.; Schaefer, F. C.; Gotthardt, H.; Brunn, E. *Tetrahedron Lett.* **1967**, 1809–1814. (b) Lira, B. F.; Athayde-Filho, P. F.; Miller, J.; Simas, A. M.; Dias, A. F.; Vieira, M. J. *Molecules* **2002**, *7*, 791–800.

(4) (a) Potts, K. T.; Houghton, E.; Husain, S. *J. Chem. Soc., Chem. Commun.* **1970**, 1025–1026. (b) Hanley, R. N.; Ollis, W. D.; Ramsden, C. A. *J. Chem. Soc., Perkin Trans. I* **1979**, 732–735. (c) Hanley, R. N.; Ollis, W. D.; Ramsden, C. A. *J. Chem. Soc., Perkin Trans. I* **1979**, 741–743. (d) Masuda, K.; Adachi, J.; Nomura, K. *J. Chem. Soc., Perkin Trans. I* **1979**, 956–959. (e) Adachi, J.; Takahata, H.; Nomura, K.; Masuda, K. *Chem. Pharm. Bull.* **1983**, *31*, 1746–1750.

(5) Araki, S.; Goto, T.; Butsugan, Y. *Bull. Chem. Soc. Jpn.* **1988**, *61*, 2977–2978.

(6) (a) Cantillo, D.; Ávalos, M.; Babiano, R.; Cintas, P.; Jiménez, J. L.; Light, M. E.; Palacios, J. C. *Org. Lett.* **2008**, *10*, 1079–1082. (b) Cantillo, D.; Ávalos, M.; Babiano, R.; Cintas, P.; Jiménez, J. L.; Light, M. E.; Palacios, J. C. *J. Org. Chem.* **2009**, *74*, 3698–3705.

To find the optimal conditions for the syntheses of **11–13**, the above-mentioned reactions were alternatively attempted under microwave irradiation, using a multimode microwave instrument (maximum power: 300 W; temperature: 100 °C measured with use of an internal fiber-optic probe) in DMF as solvent, a polar medium suitable for dielectric heating.<sup>8</sup> Under these conditions, transformations are complete within 5 min. This acceleration causes energy savings but it does not substantially affect the chemoselectivity of either of the global yields with respect to the conventional heating for the same time.<sup>9</sup> Although the conventionally heated reaction, conducted in the identical reaction vessel at 100 °C, usually requires 10–40 min for completion, we deliberately stopped these protocols after 5 min and evaluated both overall yields and selectivities (Table 1), which show a close similarity to those completed after 5 min of irradiation.

Microwave irradiation causes various thermal effects, which are clearly distinctive from those from conventional

(7) Avalos, M.; Babiano, R.; Cabanillas, A.; Cintas, P.; Higes, F. J.; Jiménez, J. L.; Palacios, J. C. *J. Org. Chem.* **1996**, *61*, 3738–3748.

(8) (a) For a recent tutorial on microwave heating and its applications in organic synthesis see: Kappe, C. O. *Chem. Soc. Rev.* **2008**, *37*, 1127–1139. (b) Perreux, L.; Loupy, A. In *Microwaves in Organic Synthesis*; Loupy, A., Ed.; Wiley-VCH: Weinheim, Germany, 2006; Chapter 4, pp 134–218. (c) For a recent and authoritative discussion on microwave apparatuses and protocols see: *Practical Microwave Synthesis for Organic Chemists. Strategies, Instruments, and Protocols*; Kappe, C. O., Dallinger, D., Murphree, S., Eds.; Wiley-VCH: Weinheim, Germany, 2008. (d) Herrero, M. A.; Kremsner, J. M.; Kappe, C. O. *J. Org. Chem.* **2008**, *73*, 36–47.

(9) Razaq, T.; Kappe, C. O. *ChemSusChem* **2008**, *1*, 123–132.

TABLE 1. Isolated Yields of Compounds 11–13 in the Reactions of Thioisomünchnones 5–7 with Aryl Isothiocyanates 8–10

entry	reactants	reaction products (% yield)				
		procedure A: CH <sub>2</sub> Cl <sub>2</sub> , rt, 24–48 h <sup>a</sup>	procedure B: DMF, rt, 12–24 h <sup>a</sup>	procedure C: DMF, 100 °C, 10–40 min <sup>a</sup>	procedure D: DMF, MW, 300 W, 100 °C, 5 min	procedure E: DMF, 100 °C, 5 min
1	5 + 8	11 (9)	11 (56)	11 (68)	11 (58)	11 (62)
2	5 + 9	11 (2) + 12 (2)	11 (21) + 12 (39)	11 (21) + 12 (37)	11 (7) + 12 (27)	11 (11) + 12 (18)
3	5 + 10	11 (44) + 13 (1)	11 (99) + 13 (1)	11 (75) + 13 (11)	11 (62) + 13 (12)	11 (70) + 13 (10)
4	6 + 8	12 (3) + 11 (2)	12 (54) + 11 (8)	12 (50) + 11 (15)	12 (52) + 11 (36)	12 (49) + 11 (15)
5	6 + 9	12 (2)	12 (32)	12 (59)	12 (56)	12 (17)
6	6 + 10	12 (38) + 13 (1)	12 (99) + 13 (1)	12 (78) + 13 (3)	12 (88) + 13 (8)	12 (64) + 13 (4)
7	7 + 8	13 (7) + 11 (27)	13 (11) + 11 (57)	13 (12) + 11 (73)	13 (5) + 11 (80)	13 (11) + 11 (70)
8	7 + 9	13 (3) + 12 (7)	13 (8) + 12 (59)	13 (7) + 12 (51)	13 (1) + 12 (73)	13 (4) + 12 (43)
9	7 + 10	13 (61)	13 (>99)	13 (91)	13 (76)	13 (88)

<sup>a</sup>The fastest reactions take place when the isothiocyanate bears an electron-withdrawing aryl substituent.

TABLE 2. Selected <sup>1</sup>H and <sup>13</sup>C Chemical Shifts (ppm) of Compounds 5–7 and 11–13

compd	<sup>1</sup> H chemical shifts			<sup>13</sup> C chemical shifts					
	N–CH <sub>2</sub>	N–CH <sub>3</sub>	O–CH <sub>3</sub>	N–CH <sub>2</sub>	N–CH <sub>3</sub>	O–CH <sub>3</sub>	C-2	C-4	C-5
5	4.23 s	2.74 s		57.7	40.0		156.2	161.2	79.8
6	4.28 s	2.79 s	3.80 s	57.6	40.0	57.6	156.5	161.3	79.9
7	4.12 s	2.64 s		58.1	40.5		155.5	161.4	79.8
11	4.28 s	2.75 s		59.1	41.5		166.6	156.8	108.0
12	4.33 s	2.80 s		59.0	41.5		166.8	156.9	108.1
13	4.30 s	2.80 s		59.5	42.0		166.8	156.1	108.6

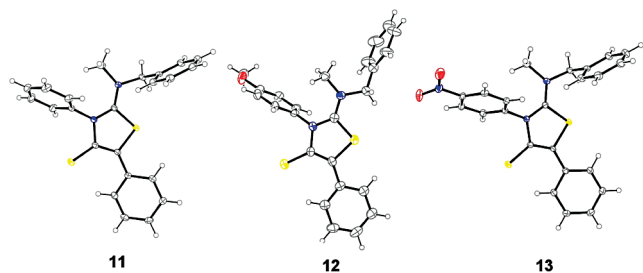


FIGURE 1. Structures of 11, 12, and 13 obtained by X-ray diffraction.

heating. Nonthermal microwave effects appear now to be flawed in the absence of experimental evidence. Leading experts have clearly evidenced that performing meaningful comparison experiments between microwaves and conventional heating requires above all accurate internal temperature measurements.<sup>8</sup> In agreement with such studies, the present results reveal that both reactivity and chemoselectivity should be considered essentially identical, within experimental errors, and not related to nonthermal effects.

It should be finally mentioned that these transformations were also attempted in CH<sub>2</sub>Cl<sub>2</sub> at 100 °C (sealed tube) under microwave irradiation. Such protocols were unsuccessful as quick and extensive decomposition of both the parent thioisomünchnone and the resulting 1,3-thiazolium-4-thiolate were observed.

It is noteworthy the extent of the influence of aryl groups, present in the thioisomünchnone and isothiocyanate partners, on the chemoselectivity of this reaction. When the aryl substituent on the isothiocyanate is more electron withdrawing than the *N*-aryl group of the thioisomünchnone, the thionation becomes the favorite pathway (entries 3 and 6, Table 1). On the other hand, the 1,3-dipolar cycloaddition route is prevalent when the more electron withdrawing aryl group is linked to the thioisomünchnone (entries 7 and 8, Table 1). A mechanistic rationale accounting for these experimental observations will be discussed later.

**Structure Characterization.** Crystalline structures of compounds 11, 12, and 13 could be satisfactorily elucidated by X-ray diffraction analyses (Figure 1).

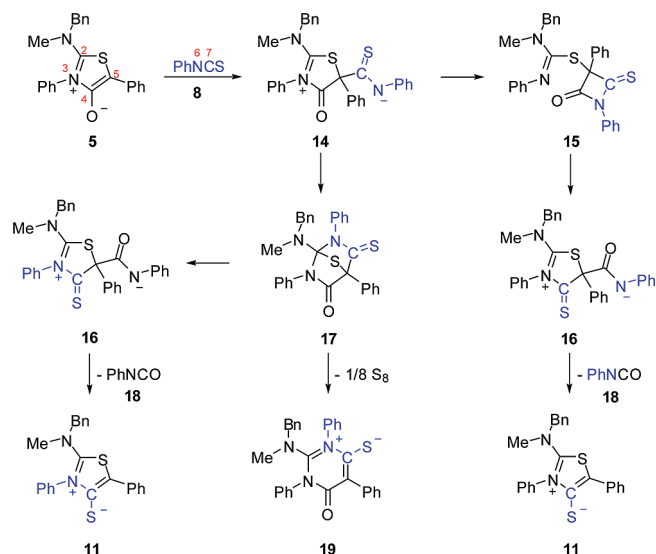
Molecular structures of 11, 12, and 13 show the perpendicular and coplanar arrangements of the mesoionic heterocycle with respect to the aryl groups linked to the N-3 and C-5 atoms, respectively. In the case of 12, suitable crystals for X-ray analysis were obtained from diethyl ether, while for compounds 11 and 13, diffraction analyses could only be accomplished after recrystallization from benzene. A salient polymorphism was observed depending on the solvent system and, remarkably, a benzene molecule is encapsulated in the crystalline lattices of compounds 11 and 13 (see the Supporting Information).

<sup>1</sup>H NMR data of compounds 11–13 are extremely simple and similar to those of the parent thioisomünchnones 5–7 (Table 2). However, the O/S exchange causes a strong deshielding ( $\Delta\delta \sim 28$  ppm) of the C-5 signal in 11–13 relative to that of compounds 5–7, while the resonances of the C-2 and C-4 carbon atoms are shifted downfield ( $\Delta\delta \sim 10.4$  ppm) and upfield (4.4–5.3 ppm), respectively. This spectroscopic behavior is analogous to that previously found for compounds 1 and 2, whose equivalent carbon atoms resonate at 151.7, 155.0, 83.9 ppm, and 160.0, 149.0, 111.0 ppm, respectively.

**Mechanistic Insights: A Theoretical Study.** In agreement with the mechanism proposed<sup>6b</sup> for the thionation of 1 and 3, the transformation of the thioisomünchnones 5–7 into 11–13 might involve a stepwise mechanism (depicted in Scheme 1 for the reaction of 5 and 8), which, in this case, could also account for the formation of product mixtures when different *N*-aryl groups are present in both reagents, the thioisomünchnone and the aryl isothiocyanate.

The overall process would be launched with the formation of an open dipolar intermediate (14) by nucleophilic addition of the C-5 heterocyclic carbon of 5 onto the thiocarbonyl carbon of the aryl isothiocyanate. Then, 14 could evolve into the azetidinic intermediate (15) by nucleophilic attack of the

**SCHEME 1. Stepwise Mechanisms for Both Thionation and 1,3-Dipolar Cycloaddition of the 1,3-Thiazolium-4-olate **5** with Phenyl Isothiocyanate (**8**)<sup>a</sup>**



<sup>a</sup>Blue is used to show the fate of the phenyl isothiocyanate moiety in the outcome of such processes.

nitrogen on the neighboring carbonyl group. The free rotation around the C–S bonds of **15** enables the isothioureidic nitrogen to be close to the thiocarbonylic carbon giving rise to a new open dipolar intermediate (**16**), which would ultimately lead to the 1,3-thiazolium-4-thiolate (**11**), the latter retaining the *N*-aryl group of the parent 1,3-thiazolium-4-olate system (**5**). Alternatively, **14** could be converted into the cycloadduct **17** by attack of the nucleophilic nitrogen on the C-2 carbon atom. The retrocycloaddition reaction of phenyl isocyanate could also lead to a 1,3-thiazolium-4-thiolate (**11**), but in this case, its *N*-phenyl group might arise from phenyl isothiocyanate (Scheme 1). In addition, the extrusion of sulfur from **17** could give rise to the betaine **19**. This substance has not been detected in these reactions, though this type of heterocyclic system was formed during the thionation of compounds **1** and **3**.

This mechanism agrees with the observed chemoselectivity, which can further be rationalized in terms of the HSAB principle. An electron-withdrawing group at the N-3 atom of a zwitterion like **14** does increase the hardness of the C-2 position, thereby favoring the formation of cycloadduct **17**, which will be especially noticeable on increasing the anion hardness with an electron-releasing group at N-6. In stark contrast, electron-withdrawing groups at N-6 significantly favor the thionation step because the anion hardness diminishes. Under such circumstances, addition to the vicinal, softer carbonyl group becomes a more favorable pathway.

Moreover, we have carried out a computational study on the global reactivity of the thioisomünchnone **5** with phenyl

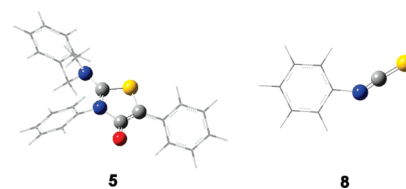


**FIGURE 2.** ONIOM[B3LYP/6-31G(d):PM3]-optimized structures for the thioisomünchnone **5** and phenyl isothiocyanate (**8**).

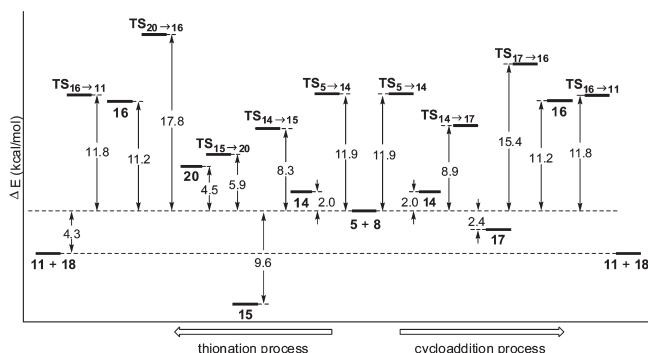
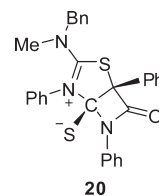


**FIGURE 3.** Energetics of the competitive thionation and cycloaddition reactions of thioisomünchnone **5** and phenyl isothiocyanate (**8**).

isothiocyanate (**8**) using the ONIOM[B3LYP/6-31G(d):PM3]<sup>10,11</sup> method. Figure 2 shows both reactants in which balls and sticks represent the partial system treated at the B3LYP/6-31G(d) level and the wire-shaped structure corresponds to the molecular fragment assessed at a semiempirical level (PM3).

Figure 3 collects the relative electronic energies of all stationary states involved in both the thionation and the 1,3-dipolar cycloaddition. Remarkably, a tetrahedral intermediate (**20**) and two saddle points (**TS<sub>15→20</sub>** and **TS<sub>20→16</sub>**) could be optimized as previous stationary points leading to **16**. An analogous tetrahedral intermediate, however, could not be obtained for the transformation of **14** into **15**.



The relative electronic energy of reactants and products points to a thermodynamically favored transformation of **5** into **11** and, from a kinetic viewpoint, the rate-determining step for both competitive processes (thionation as well as 1,3-dipolar cycloaddition) must involve formation of the open dipolar intermediate **16**. By estimating the magnitude of the two energy barriers affording **16** (17.8 and 15.4 kcal/mol) one concludes that the 1,3-dipolar cycloaddition seems to be faster than the thionation; however, experimental results (Table 1) show that the major product of each reaction depends largely on the reaction conditions and the donor/acceptor character of the aryl groups present in both reactants, thioisomünchnone and

(10) (a) Dapprich, S.; Komáromi, I.; Byun, K. S.; Morokuma, K.; Frish, M. J. *THEOCHEM* **1999**, *462*, 1–21. (b) Svensson, M.; Humbel, S.; Froese, R. D. J.; Matsubara, T.; Sieber, S.; Morokuma, K. *J. Phys. Chem.* **1996**, *100*, 19357–19363.

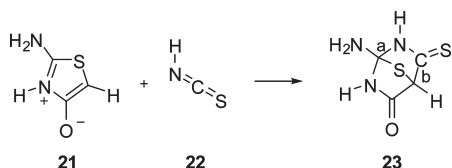
(11) Froese, R. D. J.; Morokuma, K. In *The Encyclopedia of Computational Chemistry*; Schleyer, P. v. R., Allinger, N. L., Clark, T., Gasteiger, J., Kollman, P. A., Schaefer, H. F., III, Schreiner, P. R., Eds.; John Wiley: Chichester, UK, 1998; pp 1245–1257.

**TABLE 3.** Energy Barrier Differences of the Rate-Determining Steps (Thionation Minus Cycloaddition) As a Function of the Nature of the Aryl Substituents of Both Reagents

entry	thioisomünchnone	aryl isothiocyanate	$\Delta\Delta E^\ddagger$ (kcal/mol) <sup>a</sup>
1	6	10	-4.99
2	5	10	-3.83
3	5	9	+4.84
4	7	8	+10.52
5	7	9	+11.38

<sup>a</sup>Calculated using the ONIOM[B3LYP/6-31G(d):PM3] method.

## SCHEME 2



isothiocyanate. Table 3 shows the variation in these energy barriers when the electronic nature of such aryl groups changes. Product ratios and yields reported in Table 1 are consistent with the calculated  $\Delta\Delta E^\ddagger$  values, which constitutes a sound support for the mechanism proposed (Scheme 1). Likewise, this fact validates the theoretical method at the level of theory employed, even though the aryl substituents of the whole molecular system were assessed at a semiempirical level.

At this stage, one could formulate an intriguing question, even in the absence of evidence, i.e., Does an alternative concerted mechanism for the 1,3-dipolar cycloaddition of thioisomünchnones with aryl isothiocyanates exist? To provide an unambiguous response, we decided to construct the potential energy surface (PES) for this reaction. To do it at a reasonable computational cost, we were forced to modify the structures of **5**, **8**, and **17** to generate the simplified models **21**, **22**, and **23**, which preserve the essential characteristics of the original molecules (Scheme 2). A total of 234 ( $13 \times 18$ ) full optimized [B3LYP/6-31G(d) level] structures were required to create the PES (Figure 4), stemming from the sequential lengthening (0.1 Å) of both the C–N (a) and C–C (b) bonds.

**Location of Stationary Points Along the Reaction Path.** Although at first sight the PES suggests a stepwise mechanism, a simple inspection does not allow us to establish the real location of each stationary point for this process. To make this work easier, we have come up with a suitable strategy to locate stationary points such as optimal structures (local minima) and saddle points in a reliable and unambiguous fashion.

A fitting procedure of these PES data using a Chebyshev polynomial<sup>12</sup> produces a new hypersurface with a three-dimensional representation essentially identical ( $r > 0.9999$ ) with the former (Figure 5), thereby evidencing that this polynomial constitutes the best approximation to a continuous function.

For local minima and saddle points (structures with zero gradient), the function slope and therefore its derivative equal zero. In mathematical language, it is well-known that

(12) Boyd, J. P. *Chebyshev and Fourier Spectral Methods*; Dover Publications, Inc.: Mineola, NY, 2001.

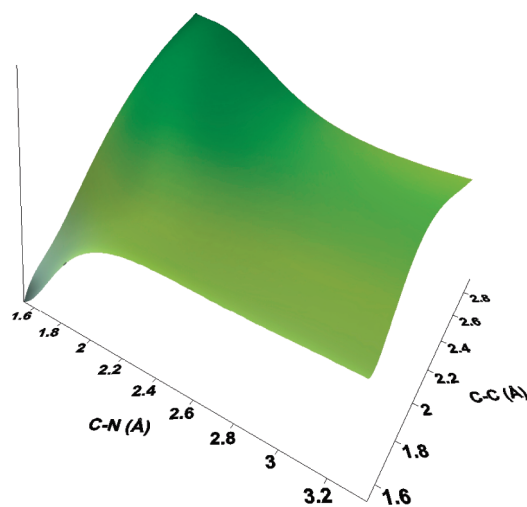


**FIGURE 4.** PES corresponding to the formation of **23** by reaction of **21** and **22**, calculated at the B3LYP/6-31G(d) level with full optimization of each structure.

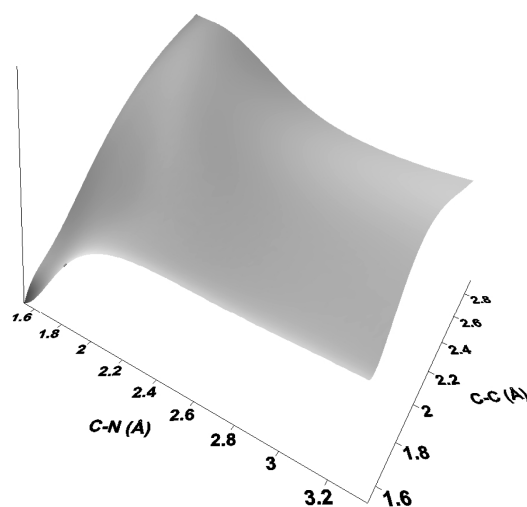


**FIGURE 5.** Three-dimensional representation of the Chebyshev polynomial that fit to the PES data of Figure 4.

such stationary points are defined as points in the two-dimensional space (surface), where

$$\frac{\partial z}{\partial x} = 0 \quad \text{and} \quad \frac{\partial z}{\partial y} = 0$$

Calculations of first derivatives with respect to either  $x$  or  $y$  coordinates and their graphical plots give rise to contour maps of isovalue lines. Colored areas can be used to depict zones where the derivative becomes close to zero ( $< 0.001$  or  $< 0.0001$ ), the lesser the derivative values the thinner the area obtained. Superposition of both plots affords intersection points, which correspond to any stationary point along the reaction path (Figure 6).

The contour maps readily identify three stationary points corresponding to two saddle points (located in blue and pink areas, which indicate C–N and C–C bond forming processes, respectively, Figure 7), plus an intermediate (in the white area, Figure 7), thus pointing to the stepwise

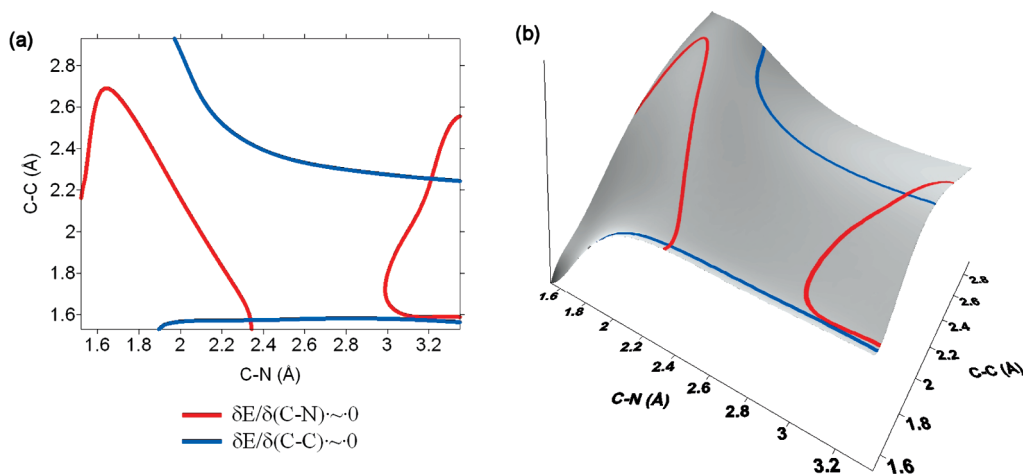


**FIGURE 6.** (a) Superposition of first derivative plots. Red and blue areas correspond to zones where the derivative values with respect to  $x$  (C–N bond) and  $y$  (C–C bond), respectively, are close to zero. (b) Superposition of first derivative plots over the Chebyshev polynomial representation.

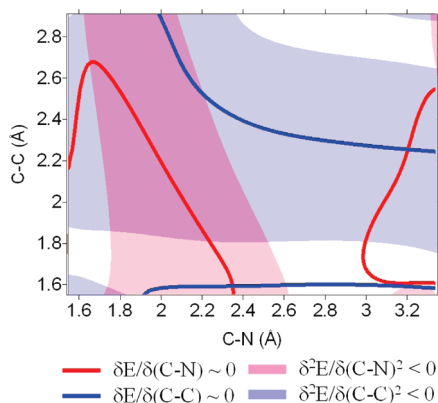


**FIGURE 7.** Superposition of first and second derivative plots. Pink and blue zones indicate concave surface areas (maxima) with respect to  $x$  and  $y$ , respectively.

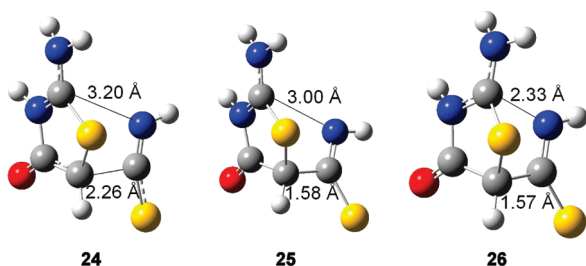


**FIGURE 8.** Full optimized structures of saddle points **24** and **26** and the open dipolar intermediate **25**.

pathway. These stationary points were further confirmed by conventional optimization and frequency analysis (Figure 8).

At this point, it should strongly be emphasized that the above methodology is not intended to replace the analytical construction of PESs, which represents a formidable task, even for very discrete species.<sup>13</sup> This rather naive protocol is

(13) For a recent revision see: Albu, T. V.; Espinosa-García, J.; Truhlar, D. G. *Chem. Rev.* **2007**, *107*, 5101–5132.

consistent with a mathematical algorithm and has proven to be both reliable and accurate in locating stationary points in numerous cycloaddition reactions.<sup>14</sup>

### Concluding Remarks

In summary, this work provides an experimental and theoretical study for the reaction of monocyclic 2-amino-1,3-thiazolium-4-olates with aryl isothiocyanates. This transformation is consistent with two competitive stepwise pathways, namely the thionation and 1,3-dipolar cycloaddition processes, which strongly depend on the substituents of the aryl groups of both reagents. Compounds **11–13** could be gratifyingly obtained as crystalline materials suitable for single-crystal diffraction analyses, after chromatographic purification (benzene–acetonitrile gradients).

While conventional reactions conducted under mild conditions are sluggish, either microwave irradiation or oil-bath heating at 100 °C in DMF represent valuable protocols from a synthetic point of view. Global reactivities and selectivities should be considered almost identical, and therefore not directly associated to the presence of the microwave field.

A hybrid ONIOM-based theoretical methodology has been performed to simulate the chemical reaction at the B3LYP/6-31G(d):PM3 level, which is consistent with experimental data. Finally, we introduce a novel and straightforward method to construct and interpret potential energy surfaces (PES) to evaluate the reaction pathways. This analysis on a simplified reaction model confirms the non-concerted nature of these reactions.

### Experimental Section

**General Procedures for the Reaction of Thioisomünchnones 5–7 with Aryl Isothiocyanates 8–10. Procedure A.** To a solution of thioisomünchnone (3 mmol) in CH<sub>2</sub>Cl<sub>2</sub> (30 mL) was added the corresponding aryl isothiocyanate (15 mmol). The reaction mixture was stirred at room temperature and monitored by TLC (benzene/acetonitrile 3:1) until the complete disappearance of

(14) We have tested the methodology in more than 30 typical cycloaddition reactions and, in all the cases, the stationary points thus obtained could further be confirmed by optimization and frequency analyses (unpublished results). The validity and extension to other organic reactions is underway.

the substrate (no more than 48 h). Then, the solvent was evaporated and the resulting crude mixture was purified by flash chromatography (benzene/acetonitrile gradient elution from 10:1 to 1:3).

**Procedure B.** In a 10-mL round flask were placed the thioisomünchnone (0.8 mmol), the corresponding aryl isothiocyanate (4 mmol), and DMF (5 mL). The mixture was stirred at room temperature until the complete disappearance of the substrate (no more than 24 h). Then, the mixture was purified by flash chromatography (benzene/acetonitrile gradient elution from 10:1 to 1:3).

**Procedure C.** In a 10-mL round flask were placed the thioisomünchnone (0.8 mmol), the corresponding aryl isothiocyanate (4 mmol), and DMF (1 mL). The mixture was heated in an oil bath at 100 °C until the complete disappearance of the substrate (no more than 40 min). Then, the mixture was cooled to room temperature and purified by flash chromatography (benzene/acetonitrile gradient elution from 10:1 to 1:3).

**Procedure D.** In a 10-mL round flask were placed the thioisomünchnone (0.8 mmol), the corresponding aryl isothiocyanate (4 mmol), and DMF (1 mL). The mixture was heated in an open vessel under microwave radiation (maximum power: 300 W) with a multimode instrument (Ethos, Advanced MW Lab-station) from Milestone, with the temperature ramping from rt to 100 °C within 1 min (using a fiber-optic probe to estimate the temperature profile). Then, the reaction was held at this temperature for 4 min. The mixture was cooled to room temperature and purified by flash chromatography (benzene/acetonitrile gradient elution from 10:1 to 1:3).

**Procedure E.** In a 10-mL round flask were placed the thioisomünchnone (0.8 mmol), the corresponding aryl isothiocyanate (4 mmol), and DMF (1 mL). The mixture was heated in an oil bath at 100 °C for 5 min. Then, the mixture was cooled to room temperature and purified by flash chromatography (benzene/acetonitrile gradient elution from 10:1 to 1:3).

The complete set of conventional (36 reactions) and micro-waved (9 reactions) transformations has been carried out following the above procedures A–D and E, respectively. Their product distribution and yields are listed in Table 1. Analytical data of compounds **11–13** are as follows.

**2-(*N*-Methylbenzylamino)-3,5-diphenyl-1,3-thiazolium-4-thiolate (11):** mp 158–159 °C; <sup>1</sup>H NMR (400 MHz, CDCl<sub>3</sub>) δ 8.30

(dd, 2H, *J* = 0.8, 8.4 Hz), 7.46 (t, 3H, *J* = 7.2 Hz), 7.34 (m, 7H), 7.18 (t, 1H, *J* = 7.2 Hz), 7.01 (dd, 2H, *J* = 2.4, 7.6 Hz), 4.28 (s, 2H), 2.75 (s, 3H); <sup>13</sup>C NMR (100 MHz, CDCl<sub>3</sub>) δ 166.6, 156.8, 138.4, 133.5, 129.9, 129.5, 129.3, 129.1, 128.5, 128.3, 128.2, 127.1, 126.7, 126.0, 108.0, 59.1, 41.5. Anal. Calcd for C<sub>23</sub>H<sub>20</sub>N<sub>2</sub>S<sub>2</sub>·<sup>1</sup>/<sub>2</sub>C<sub>6</sub>H<sub>6</sub>: C, 73.03; H, 5.42; N, 6.55; S, 15.00. Found: C, 72.75; H, 5.68; N, 6.77; S, 14.72.

**3-(4-Methoxyphenyl)-2-(*N*-methylbenzylamino)-5-phenyl-1,3-thiazolium-4-thiolate (12):** mp 156–157 °C; <sup>1</sup>H NMR (400 MHz, CDCl<sub>3</sub>) δ 8.29 (dd, 2H, *J* = 0.8, 8.4 Hz), 7.34 (m, 5H), 7.28 (d, 2H, *J* = 9.2 Hz), 7.18 (t, 1H, *J* = 7.2 Hz), 7.03 (dd, 2H, *J* = 2.4, 8.0 Hz), 6.96 (dd, 2H, *J* = 2.4, 6.8 Hz), 4.33 (s, 2H), 3.81 (s, 3H), 2.80 (s, 3H); <sup>13</sup>C NMR (100 MHz, CDCl<sub>3</sub>) δ 166.8, 160.3, 133.7, 133.5, 130.8, 130.5, 129.1, 128.5, 128.2, 127.0, 126.7, 126.0, 114.5, 59.0, 55.5, 41.5. Anal. Calcd for C<sub>24</sub>H<sub>22</sub>N<sub>2</sub>OS<sub>2</sub>·<sup>1</sup>/<sub>2</sub>C<sub>6</sub>H<sub>6</sub>: C, 70.86; H, 5.51; N, 6.12; S, 14.01. Found: C, 70.64; H, 5.37; N, 6.39; S, 14.22.

**2-(*N*-Methylbenzylamino)-3-(4-nitrophenyl)-5-phenyl-1,3-thiazolium-4-thiolate (13):** mp 145–146 °C; <sup>1</sup>H NMR (400 MHz, CDCl<sub>3</sub>) δ 8.28 (dd, 2H, *J* = 1.2, 8.4 Hz), 8.23 (d, 2H, *J* = 8.8 Hz), 7.58 (d, 2H, *J* = 8.8 Hz), 7.38 (t, 2H, *J* = 7.6 Hz), 7.33 (t, 3H, *J* = 3.2 Hz), 7.22 (t, 1H, *J* = 7.2 Hz), 6.58 (m, 2H), 4.30 (s, 2H), 2.80 (s, 3H); <sup>13</sup>C NMR (100 MHz, CDCl<sub>3</sub>) δ 166.8, 156.1, 148.1, 143.5, 133.1, 132.9, 131.0, 129.3, 128.9, 128.4, 126.8, 126.6, 126.4, 124.3, 108.6, 59.5, 42.0. Anal. Calcd for C<sub>23</sub>H<sub>19</sub>N<sub>3</sub>O<sub>2</sub>S<sub>2</sub>·<sup>2</sup>/<sub>3</sub>C<sub>6</sub>H<sub>6</sub>: C, 66.78; H, 4.77; N, 8.65; S, 13.21. Found: C, 66.51; H, 5.03; N, 8.48; S, 12.89.

**Acknowledgment.** This work was supported by the Ministerio de Educación y Ciencia and FEDER (CTQ2007-66641) and the Junta de Extremadura (PRI07A016 and PRI08A032). One of us (D.C.) thanks the Spanish Ministerio de Educación y Ciencia for a fellowship.

**Supporting Information Available:** <sup>1</sup>H and <sup>13</sup>C NMR spectra for compounds **11–13**, crystal data for compounds **11–13** in CIF format, and computational data for all structures computed at the ONIOM[B3LYP/6-31G(d):PM3] level. This material is available free of charge via the Internet at <http://pubs.acs.org>.